

# Norwood procedure with non-valved right ventricle to pulmonary artery shunt improves ventricular energetics despite the presence of diastolic regurgitation: a theoretical analysis

Shuji Shimizu · Dai Une · Toshiaki Shishido ·  
Atsunori Kamiya · Toru Kawada · Shunji Sano ·  
Masaru Sugimachi

Received: 17 May 2011 / Accepted: 10 July 2011 / Published online: 10 August 2011  
© The Physiological Society of Japan and Springer 2011

**Abstract** When the Norwood procedure is conducted for the hypoplastic left heart syndrome using a non-valved right ventricle (RV) to pulmonary artery (PA) shunt, diastolic regurgitation from PA to RV may have an adverse effect on postoperative hemodynamics. In this study, we examined the impact of the diastolic regurgitation on ventricular energetics by computational analysis using a combination of a time-varying elastance chamber model and a modified three-element Windkessel vascular model. This study revealed that use of the valved or non-valved RV-PA shunt eliminated pulmonary over-circulation which was observed when using the systemic to pulmonary artery shunt (modified Blalock–Taussig shunt). Although the valved RV-PA shunt improved pulmonary blood supply and consequently increased pulmonary artery flow and oxygen saturation compared to the non-valved RV-PA shunt, the non-valved RV-PA shunt improved ventricular energetics in spite of the presence of PA to RV regurgitation.

**Keywords** Hypoplastic left heart syndrome · Norwood procedure · Right ventricle to pulmonary artery shunt · Ventricular energetics · Valved · Computational model

## Introduction

The outcome of the Norwood procedure for hypoplastic left heart syndrome (HLHS) has improved in the past several decades. Previously, pulmonary circulation was maintained by a systemic to pulmonary artery shunt (SPS), such as the modified Blalock–Taussig shunt. However, the SPS has the drawback of systemic-to-pulmonary diastolic run-off, which causes a massive increase in ventricular preload. The development of the right ventricle to pulmonary artery (RV-PA) shunt may have contributed to the dramatic improvement in clinical outcome of recent years, because the RV-PA shunt eliminates the diastolic run-off and increases diastolic systemic arterial pressure (SAP). This increase in diastolic SAP may improve coronary blood supply [1]. Furthermore, the RV-PA shunt may reduce myocardial oxygen demand. Bove et al. [2] reported that the RV-PA shunt decreased stroke work and improved right ventricular energetics.

The RV-PA shunt may be classified into valved and non-valved. The non-valved RV-PA shunt is associated with diastolic regurgitation from PA to RV. This regurgitation may increase RV preload and myocardial oxygen demand compared to the valved RV-PA shunt. Therefore, preventing diastolic regurgitation using the valved conduit may further improve clinical outcome. Reihartz et al. [3] reported that use of a homograft valved RV-PA conduit was associated with low early mortality. Takeuchi et al. [4] used a valved saphenous vein homograft and also reported improved right ventricular function. However, whether the non-valved RV-PA shunt truly improves the outcome of the Norwood procedure compared to the SPS, and whether the valved RV-PA shunt further improves the outcome compared to the non-valved RV-PA shunt remain controversial.

S. Shimizu (✉) · D. Une · T. Shishido · A. Kamiya ·  
T. Kawada · M. Sugimachi  
Department of Cardiovascular Dynamics,  
National Cerebral and Cardiovascular Center Research Institute,  
5-7-1 Fujishiro-dai, Suita, Osaka 565-8565, Japan  
e-mail: shujismz@ri.ncvc.go.jp

S. Shimizu · S. Sano  
Department of Cardiovascular Surgery, Okayama University  
Graduate School of Medicine, Dentistry and Pharmaceutical  
Sciences, Okayama, Japan

This study aimed to clarify the impact of diastolic regurgitation from PA to RV on ventricular energetics by conducting a theoretical analysis using computational models.

**Methods**

We modeled the cardiovascular systems of the Norwood procedure using the SPS, and valved and non-valved RV-PA shunts. The electrical analogs of the models used to simulate the cardiovascular systems are shown in Fig. 1. We modeled the postoperative cardiovascular systems mathematically by a combination of the time-varying

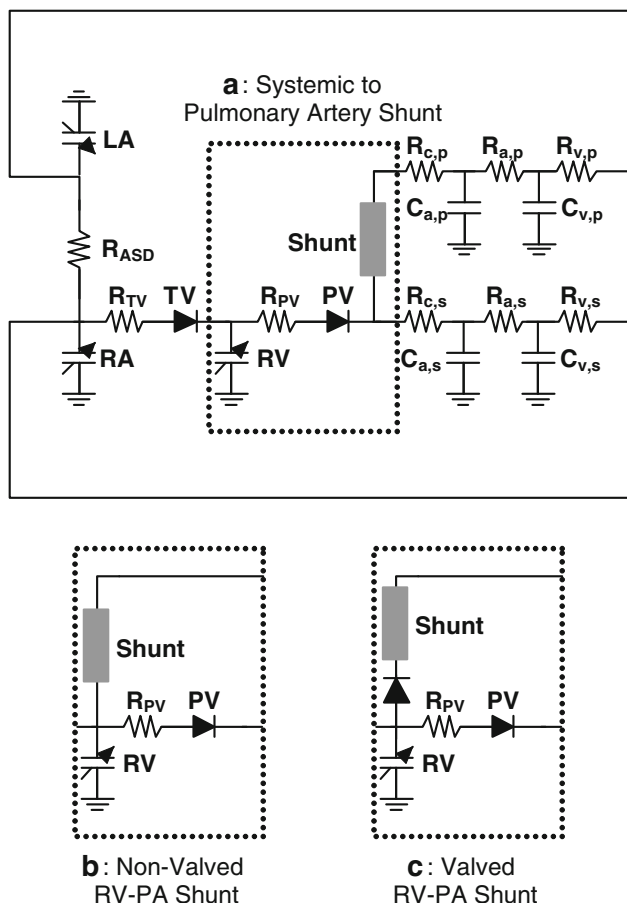


**Fig. 1** Electrical analogs of Norwood procedures. **a** Norwood procedure with systemic to pulmonary shunt, **b** Norwood procedure with non-valved right ventricle to pulmonary artery (RV-PA) shunt, **c** Norwood procedure with valved RV-PA shunt. LA left atrium, RA right atrium, RV right ventricle, PV pulmonary valve, TV tricuspid valve, ASD atrial septal defect.  $R_a$  arterial resistance,  $R_c$  characteristic impedance,  $R_v$  venous resistance,  $C_a$  arterial capacitance,  $C_v$  venous capacitance. *s* and *p* systemic and pulmonary circulation, respectively.  $R_{PV}$ ,  $R_{TV}$  and  $R_{ASD}$  resistance at PV, TV and ASD, respectively

elastance cardiac chamber model and the three-element Windkessel vascular model.

**Heart**

The right ventricular and atrial chambers are represented by the time-varying elastance model [5–7]. The end-systolic pressure–volume relationship is described by a linear equation:

$$P_{es,cc} = E_{es,cc}[V_{es,cc} - V_{0,cc}] \tag{1}$$

where  $P_{es,cc}$  is end-systolic pressure,  $V_{es,cc}$  is end-systolic volume,  $E_{es,cc}$  is the maximal volume elastance,  $V_{0,cc}$  is the volume at which end-systolic pressure is equal to 0 mmHg, and cc denotes the right atrial (RA), left atrial (LA), or right ventricular (RV) chamber. The end-diastolic pressure–volume relationship is represented by a non-linear equation:

$$P_{ed,cc} = A_{cc}[e^{B_{cc}(V_{ed,cc}-V_{0,cc})} - 1] \tag{2}$$

where  $P_{ed,cc}$  is end-diastolic pressure,  $V_{ed,cc}$  is end-diastolic volume,  $A_{cc}$  and  $B_{cc}$  are constants [5–7]. We assumed the time course of elastance by defining normalized elastance curve  $e_{cc}(t)$  as follows:

$$e_{cc}(t) = 0.5 [1 - \cos(\pi t / T_{es,cc})] \quad (0 \leq t < 2T_{es,cc})$$

$$e_{cc}(t) = 0 \quad (2T_{es,cc} \leq t < T_c) \tag{3}$$

where  $t$  is the time from the start of systole,  $T_{es,cc}$  is the time to the end of systole, and  $T_c$  is the duration of cardiac cycle. Using  $e_{cc}(t)$ , the instantaneous pressure–volume relationship is described by:

$$P_{cc}(t) = [P_{es,cc}(V_{cc}) - P_{ed,cc}(V_{cc})]e_{cc}(t) + P_{ed,cc}(V_{cc}) \tag{4}$$

Ventricular systole is preceded by atrial systole. The time advance of atrial systole (DT) is calculated as a fixed fraction of  $T_c$  ( $DT = 0.02 T_c$ ) [9]. The function of each chamber is characterized by the parameters  $E_{es,cc}$ ,  $T_{es,cc}$ ,  $V_{0,cc}$ ,  $A_{cc}$ ,  $B_{cc}$  and  $e_{cc}(t)$ . The same  $e_{cc}(t)$  is used for all chambers, but the other parameters are different between chambers, as shown in Table 1. Nonrestrictive atrial septal defect is described as constant resistance ( $R_{ASD}$ ). Each valve is represented as an ideal diode connected serially to a small resistor (pulmonary  $R_{PV}$ , tricuspid  $R_{TV}$ ).

**Vascular system**

Basically, the pulmonary and systemic circulations are modeled as modified Windkessel impedances. Each vascular system is modeled by lumped venous ( $C_v$ ) and arterial ( $C_a$ ) capacitances, a characteristic impedance ( $R_c$ ) that is related to the stiffness of the proximal aorta or pulmonary artery, a lumped arterial resistance ( $R_a$ ), and a

**Table 1** Parameters used in modeling

Heart rate (HR) (beats/min)	160		
Duration of cardiac cycle ( $T_c$ ) (ms)	375		
Time to end systole ( $T_{es}$ ) (ms)	RV: 136	RA: 56	LA: 56
End-systolic elastance ( $E_{es}$ ) (mmHg/ml)	RV: 8.5	RA: 7.35	LA: 7.35
Scaling factor of EDPVR ( $A$ ) (mmHg)	RV: 0.9	RA: 0.17	LA: 0.17
Exponent for EDPVR ( $B$ ) ( $\text{ml}^{-1}$ )	RV: 0.062	RA: 0.484	LA: 0.484
Unstressed volume ( $V_0$ ) (ml)	RV: 4	RA: 1	LA: 1
Valvular resistance (forward) ( $\text{mmHg s ml}^{-1}$ )	Pulmonary: 0.0004	Tricuspid: 0.00004	
Resistance ( $\text{mmHg s ml}^{-1}$ )	ASD: 0.001		
Index of pure viscous effects ( $k_1$ ) [ $\text{mmHg (l/s)}^{-1} \text{mm}^4$ ]	Shunt: $5.76 \times 10^4$		
Index of convective acceleration ( $k_2$ ) [ $\text{mmHg (l/s)}^{-2} \text{mm}^4$ ]	Shunt: $1.87 \times 10^7$		
Arterial resistance ( $R_a$ ) ( $\text{mmHg s ml}^{-1}$ )	Systemic (s): 3.83	Pulmonary (p): 0.63	
Characteristic impedance ( $R_c$ ) ( $\text{mmHg s ml}^{-1}$ )	Systemic (s): 0.20	Pulmonary (p): 0.028	
Venous resistance ( $R_v$ ) ( $\text{mmHg s ml}^{-1}$ )	Systemic (s): 0.083	Pulmonary (p): 0.011	
Arterial capacitance ( $C_a$ ) (ml/mmHg)	Systemic (s): 0.50	Pulmonary (p): 0.31	
Venous capacitance ( $C_v$ ) (ml/mmHg)	Systemic (s): 4.39	Pulmonary (p): 0.89	

RV right ventricle, RA right atrium, LA left atrium, EDPVR end-diastolic pressure–volume relation, ASD atrial septal defect

resistance proximal to  $C_v$  ( $R_v$ ). This framework is similar to that used in deriving Guyton’s resistance to venous return [8]. Arterial and venous capacitors for systemic circulation are denoted by  $C_{a,s}$  and  $C_{v,s}$ , respectively, and those for pulmonary circulation by  $C_{a,p}$  and  $C_{v,p}$ . The ratio of  $C_a$  to  $C_v$  is obtained from previous reports [6, 9, 10].

The relation between pressure ( $P_c$ ) and volume ( $V_c$ ) in each capacitance is described by the following linear equation:

$$P_c = \frac{V_c}{C} \tag{5}$$

The change in volume in each capacitance [ $dV(t)/dt$ ] is described by the differential equation below:

$$\frac{dV(t)}{dt} = \sum Q_{\text{inflow}}(t) - \sum Q_{\text{outflow}}(t) \tag{6}$$

where  $Q_{\text{inflow}}(t)$  and  $Q_{\text{outflow}}(t)$  indicate the instantaneous volumetric flow rates at the inlet and outlet, respectively, of each compartment.

#### Pressure drop across the shunt

Flow of non-Newtonian fluid in a curved pipe is approximated as a quadratic function of  $Q(t)$  [11, 12]. The instantaneous pressure drop across the shunt is described by:

$$\Delta P(t) = \frac{k_1 Q(t) + k_2 Q^2(t)}{D^4} \tag{7}$$

where  $\Delta P(t)$  (mmHg) is pressure drop across the shunt,  $Q(t)$  (l/s) is the instantaneous volume flow rate in shunt,  $D$  (mm) is the shunt diameter,  $k_1$  [ $\text{mmHg (l/s)}^{-1} \text{mm}^4$ ]

is the index of pure viscous effects and  $k_2$  [ $\text{mmHg (l/s)}^{-2} \text{mm}^4$ ] is the index of convective acceleration [9].

#### Protocols

First, the control state was simulated using the 4.0-mm SPS model. Total stressed blood volume ( $V_s$ ), which is the sum of the stressed volumes in all capacitances and in all chambers, was set as 80 ml.

$$V_s = V_{RV} + V_{LA} + V_{RA} + V_{C_{a,s}} + V_{C_{v,s}} + V_{C_{a,p}} + V_{C_{v,p}} \tag{8}$$

We solved the simultaneous differential equations (Eqs. 1–8) using MATLAB (MathWorks).

Shunt diameter ( $D$ ) was decreased stepwise from 4.0 to 3.0 mm at decrements of 0.5 mm in the SPS model and increased from 4.0 to 6.0 mm at increments of 1.0 mm in both the valved and non-valved RV-PA shunt models. RV forward flow, systemic and pulmonary flows ( $Q_s$  and  $Q_p$ ), systemic and pulmonary arterial pressures (SAP and PAP), right ventricular end-diastolic volume (RVEDV), stroke work (SW), systolic pressure–volume area (PVA) and mechanical efficiency after each procedure were calculated for each shunt diameter. Heart rate and mean SAP were set at the same values as those of the control state, by adjusting the total stressed blood volume ( $V_s$ ).

#### Calculation of arterial and venous oxygen saturation

Since the total amount of  $O_2$  present in the atrium is preserved and the decrease in  $O_2$  content in blood balances the whole body  $O_2$  consumption, arterial ( $SaO_2$ ) and venous  $O_2$  saturation ( $SvO_2$ ) are calculated by the following equations for  $Q_p$  and  $Q_s$  (l/min):

$$SaO_2 = S_{pV}O_2 - \frac{CVO_2 \times BSA}{1.34 \times Hb \times 10 \times Q_p}$$

$$SvO_2 = SaO_2 - \frac{CVO_2 \times BSA}{1.34 \times Hb \times 10 \times Q_s}$$

where  $S_{pV}O_2$  is the pulmonary venous  $O_2$  saturation,  $CVO_2$  ( $ml\ O_2/min/m^2$ ) is the whole body  $O_2$  consumption,  $BSA$  ( $m^2$ ) is the body surface area, and  $Hb$  ( $g/dl$ ) is the hemoglobin concentration. The constant 10 ( $dl/l$ ) converts l to dl, and 1.34 ( $ml\ O_2/g$ ) converts hemoglobin content to oxygen content. The following assumptions are used in the  $O_2$  calculation:  $S_{pV}O_2 = 0.97$  (dimensionless),  $CVO_2 = 185\ ml\ O_2/min/m^2$ ,  $BSA = 0.20\ m^2$  and  $Hb = 16.0\ g/dl$  [9, 13].

## Results

The hemodynamic parameters obtained from the computational simulations are shown in Table 2.

Although the increase in shunt diameter caused an increase in systolic SAP and a decrease in diastolic SAP in the SPS model, changes in shunt diameter only affect systolic and diastolic SAP slightly in both the valved and non-valved RV-PA shunt models. Despite the use of small caliber shunt in the SPS model, mean PAP,  $Q_p$  and  $Q_p/Q_s$

were higher than in both valved and non-valved RV-PA shunt models. Mean PAP,  $Q_p$  and  $Q_p/Q_s$  in the 3.5-mm SPS model were higher than those in the 6.0-mm non-valved RV-PA shunt model and almost equivalent to those in the 5.0-mm valved RV-PA shunt model.

Right ventricular pressure, SAP, PAP, aortic flow, and shunt flow in the 3.5-mm SPS, 6.0-mm non-valved shunt, and 5.0-mm valved RV-PA shunt models are shown in Fig. 2. In both valved and non-valved RV-PA shunt models, RV ejection to pulmonary circulation through the shunt preceded RV ejection to systemic circulation and continued even after the end of ejection to systemic circulation. Comparisons of the hemodynamics of the 3.5-mm SPS, and 5.0-mm valved and 6.0-mm non-valved RV-PA shunt models are shown in Fig. 3. RVEDV was smaller in the 6.0-mm non-valved RV-PA shunt ( $-3.7\%$ ) and the 5.0-mm valved RV-PA shunt ( $-11.7\%$ ) models than that in the 3.5-mm SPS model. At the same shunt diameter, mean PAP,  $Q_p$ ,  $Q_p/Q_s$ ,  $SaO_2$  and  $SvO_2$  were higher with the valved RV-PA shunt than with the non-valved shunt.

In the SPS model, the use of a larger conduit significantly increased systemic-to-pulmonary diastolic run-off and RVEDV (Table 2). In the valved and non-valved RV-PA shunt models, increase in conduit size likewise

**Table 2** Hemodynamic data obtained from computational simulation of SPS, non-valved RV-PA shunt, and valved RV-PA shunt

	Mathematical models								
	SPS			Non-valved RV-PA			Valved RV-PA		
	3.0	3.5	4.0	4.0	5.0	6.0	4.0	5.0	6.0
Shunt diameter (mm)	3.0	3.5	4.0	4.0	5.0	6.0	4.0	5.0	6.0
Heart rate (beats/min)	160			160			160		
Systolic systemic artery pressure (mmHg)	83.9	87.0	90.9	75.7	76.3	77.0	75.7	76.2	76.9
Diastolic systemic artery pressure (mmHg)	46.6	45.0	43.4	51.9	51.9	51.9	51.9	51.8	51.9
Mean systemic artery pressure (mmHg)	58.6	58.7	58.7	58.7	58.7	58.7	58.7	58.7	58.7
Mean PA pressure (mmHg)	10.4	13.8	17.3	7.50	9.83	11.9	8.98	12.6	16.2
RV forward flow (l/min)	1.60	1.86	2.14	1.53	1.86	2.19	1.51	1.81	2.10
$Q_p$ (l/min)	0.77	1.04	1.32	0.55	0.73	0.90	0.68	0.98	1.27
$Q_s$ (l/min)	0.83	0.82	0.82	0.83	0.83	0.83	0.83	0.83	0.83
$Q_p/Q_s$	0.94	1.26	1.62	0.66	0.88	1.09	0.81	1.18	1.54
Diastolic run-off (l/min)	0.52	0.69	0.85						
Diastolic regurgitation (l/min)				0.15	0.29	0.47			
$SaO_2$ (%)	74.7	80.4	83.9	65.4	73.5	77.8	71.5	79.3	83.4
$SvO_2$ (%)	53.9	59.5	62.8	44.8	52.8	56.9	50.8	58.5	62.5
Stressed blood volume (ml)	70.6	75.1	80.0	64.9	67.9	71.4	65.7	69.2	73.2
RVEDV (ml)	21.6	23.3	25.0	19.4	20.8	22.4	19.3	20.6	22.0
Stroke work (mmHg ml)	759	905	1,062	600	713	829	596	704	815
Systolic PVA (mmHg ml)	1,008	1,157	1,315	765	851	949	762	843	934
Mechanical efficiency (%)	75.3	78.2	80.8	78.4	83.8	87.4	78.3	83.5	87.2

SPS systemic to pulmonary artery shunt, RV-PA right ventricle to pulmonary artery shunt, RV right ventricle, PA pulmonary artery,  $Q_p$  pulmonary blood flow,  $Q_s$  systemic blood flow,  $SaO_2$  arterial oxygen saturation,  $SvO_2$  venous oxygen saturation, RVEDV right ventricular end-diastolic volume, PVA systolic pressure–volume area

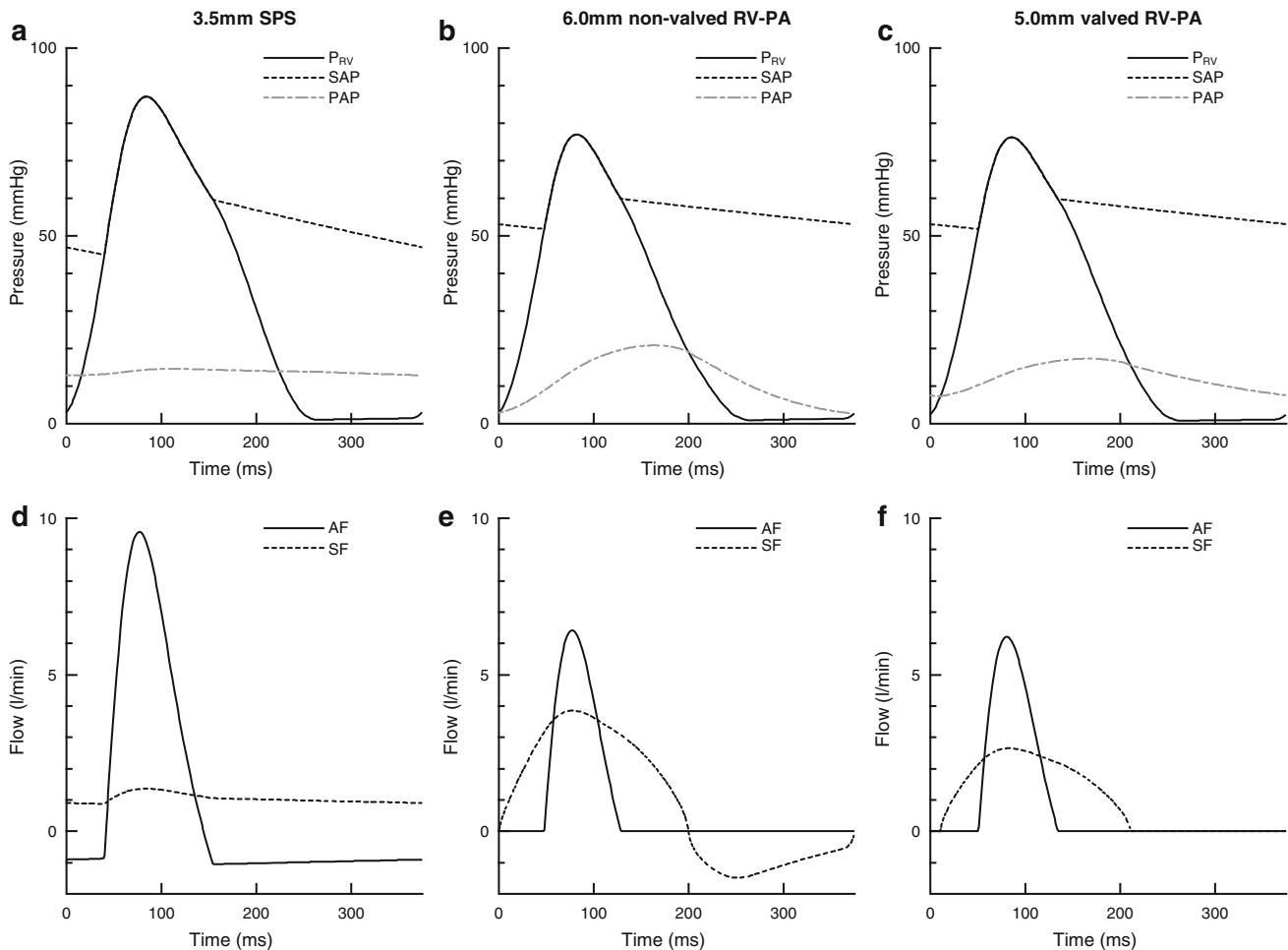


**Fig. 2** Right ventricular pressure, systemic and pulmonary arterial pressures, aortic flow and shunt flow computed from the mathematical models of Norwood procedures with 3.5-mm systemic to pulmonary artery shunt (SPS **a**, **d**), 6.0-mm non-valved right ventricle to

pulmonary artery (RV-PA) shunt (**b**, **e**), and 5.0-mm valved RV-PA shunt (**c**, **f**).  $P_{RV}$  right ventricular pressure, SAP systemic arterial pressure, PAP pulmonary arterial pressure, AF aortic flow, SF shunt flow

increased RVEDV, but the magnitudes were smaller than those of the SPS model, despite larger conduits being used in these models. The smaller RVEDV contributed to decreases in SW and PVA. The pressure–volume loops of the 3.5-mm SPS, and the 5.0-mm valved and 6.0-mm non-valved RV-PA shunt models are shown in Fig. 4. The SW in the 5.0-mm valved and 6.0-mm non-valved RV-PA shunts were  $-22.3$  and  $-8.4\%$ , respectively, smaller than that in the 3.5-mm SPS. The PVA in the 5.0-mm valved and 6.0-mm non-valved RV-PA shunts were  $-27.1$  and  $-18.0\%$ , respectively, smaller than that in the 3.5-mm SPS. Mechanical efficiency (SW/PVA) in the 5.0-mm valved and 6.0-mm non-valved RV-PA shunt were 5.3 and 9.2%, respectively, higher than that in the 3.5-mm SPS. Although the use of non-valved conduit caused diastolic regurgitation from PA to RV, there was no difference in mechanical efficiency between the valved and non-valved RV-PA shunts at the same shunt diameter. Furthermore, compared to the SPS and the valved RV-PA shunt, the non-valved

RV-PA shunt delivered the highest mechanical efficiency at any given  $Q_p/Q_s$  (Fig. 5).

**Discussion**

The Norwood procedure for stage I palliation of the HLHS was first reported in 1983 [14]. In the conventional Norwood procedure, pulmonary circulation was maintained by a SPS, such as the modified Blalock–Taussig shunt. The development of the RV-PA shunt in the last decade has improved patient’s mortality and morbidity [15]. Since Sano et al. [16] reported their experience with the non-valved RV-PA shunt in 2003, this modification has been widely used. However, it remains controversial whether the RV-PA shunt truly improves the outcome of the Norwood procedure.

The RV-PA shunt eliminates systemic to pulmonary diastolic run-off that occurs when using the SPS, which

**Fig. 3** Hemodynamics obtained from the 3.5-mm systemic-to-pulmonary shunt (SPS) model, and 6.0-mm non-valved and 5.0-mm valved right ventricle to pulmonary artery (RV-PA) shunt models

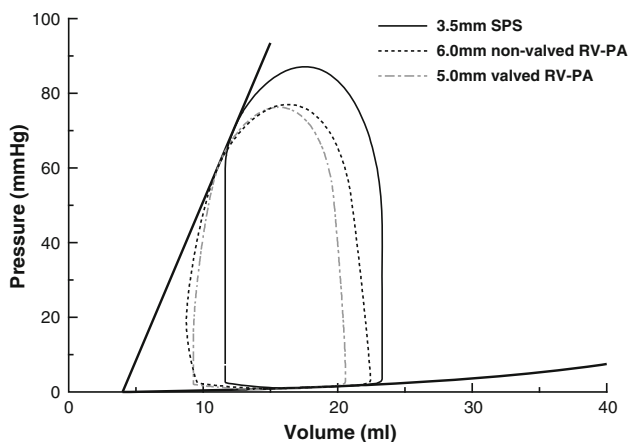
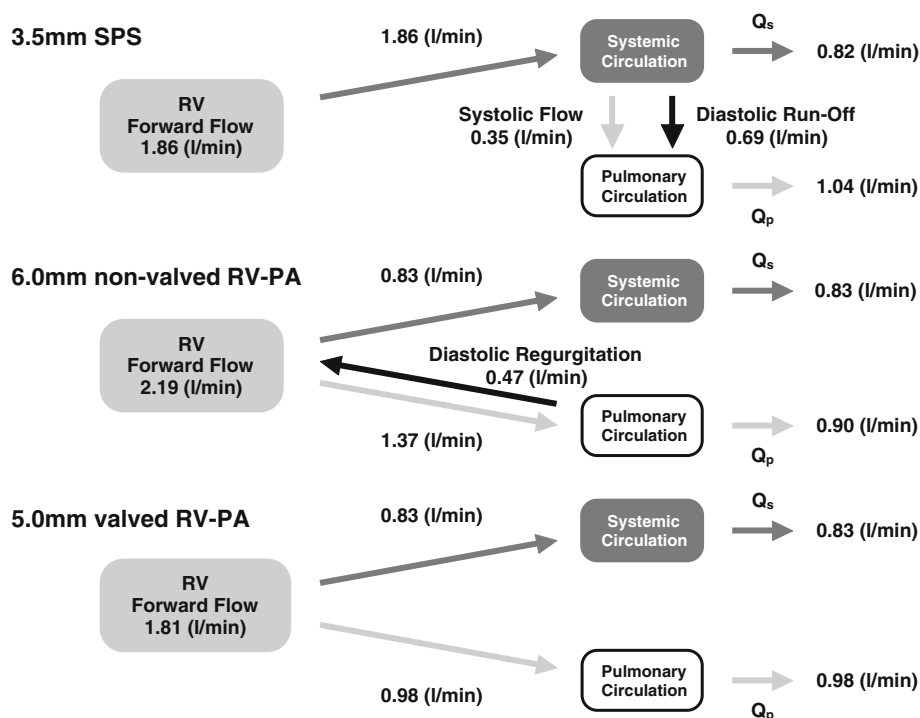


**Fig. 4** Pressure-volume loops of simulated Norwood procedures. *Solid line* 3.5-mm systemic to pulmonary artery shunt (SPS), *dotted line* 6.0-mm non-valved right ventricle to pulmonary artery (RV-PA) shunt, *dot-dashed line* 5.0-mm valved RV-PA shunt

causes a massive increase in ventricular preload. However, diastolic regurgitation from PA to RV is a drawback of the non-valved RV-PA shunt. Thus, some authors have reported the advantages of a valved RV-PA shunt [3, 4, 17]. Use of a valved RV-PA shunt prevents diastolic regurgitation from PA to RV, and should further decrease ventricular preload. However, the present theoretical study based on mathematical models revealed that the valved RV-PA shunt mainly improves pulmonary blood supply and the favorable effect on ventricular energetics is equivalent to that of the non-valved RV-PA shunt.

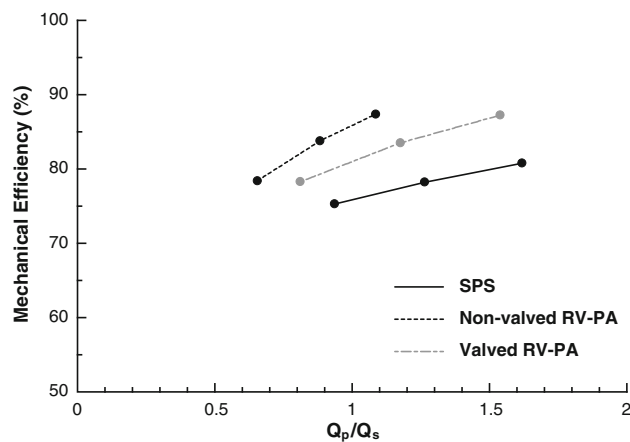


**Fig. 5** The relation between  $Q_p/Q_s$  and mechanical efficiency. *Solid line* systemic to pulmonary artery shunt (SPS), *dotted line* non-valved right ventricle to pulmonary artery (RV-PA) shunt, *dot-dashed line* valved RV-PA shunt

#### Influence on systemic circulation

In the SPS model, the use of a larger caliber shunt increased systolic SAP and decreased diastolic SAP. In both the valved and non-valved RV-PA shunt models, however, systolic and diastolic SAP did not change with the increase in shunt diameter. Diastolic SAP in both RV-PA shunt models were at most 8 mmHg higher than that in the SPS model. Some clinical reports have already demonstrated lower diastolic SAP using the SPS [18, 19]. Lower diastolic SAP may decrease coronary perfusion



pressure and result in coronary malperfusion. Therefore, excessive decrease in diastolic SAP when using the SPS may cause global myocardial ischemia and impair the postoperative surgical outcome. On the other hand, higher and stable diastolic SAP with both the valved and non-valved RV-PA shunts is favorable for myocardial blood supply.

#### Influence on pulmonary circulation

The  $Q_p$  was excessively high in the SPS model, but was lower in both the valved and non-valved RV-PA shunt models. The  $Q_p$  in the 3.5-mm SPS model was similar to that in the 5.0-mm valved RV-PA shunt and higher than that in the 6.0-mm non-valved RV-PA shunt model. The RV-PA shunts contributed to avoiding pulmonary over-circulation and maintaining appropriate pulmonary blood supply in spite of the larger conduits.

In the present study, the valved RV-PA shunt eliminated diastolic regurgitation from PA to RV, and improved pulmonary blood supply compared to the non-valved RV-PA shunt. At the same shunt diameter,  $Q_p$  was at most 42% higher in the valved RV-PA shunt than in the non-valved RV-PA shunt model. This resulted in higher oxygen saturation in the valved RV-PA shunt. To obtain the same  $Q_p$  as the valved RV-PA shunt, a non-valved RV-PA shunt may require larger stressed blood volume and may cause the increase in ventricular preload. Since some authors reported decreased SvO<sub>2</sub> as a predictor of morbidity after the Norwood procedure [20, 21], the valved RV-PA shunt that yields higher SvO<sub>2</sub> may be favorable for pulmonary circulation.

Caspi et al. [22] suggested that the Norwood procedure with RV-PA conduit may have favorable effects on the development of the pulmonary artery, which may be associated with the pulsatile pulmonary flow. The importance of pulsatility for the growth of pulmonary artery has been reported [23, 24]. The smaller pulsatility of pulmonary flow in the SPS as shown in Fig. 2d may impair the development of the pulmonary artery.

#### Influence on RVEDV

The RVEDV was markedly reduced in both the non-valved and valved RV-PA shunt models compared to the SPS model. When using a SPS, systemic and pulmonary arteries are directly connected. Therefore, a blood shift from systemic to pulmonary circulation in the diastolic phase (diastolic run-off) cannot be avoided, because pulmonary vascular resistance is usually lower than systemic vascular resistance. This should cause a decrease in systemic arterial pressure and require a greater stressed blood volume to maintain the mean SAP (Table 2), resulting in increased

RVEDV and  $Q_p$ . When the RV-PA shunts are used, since systemic and pulmonary arteries originate separately from the RV, diastolic run-off is avoided and RVEDV and  $Q_p$  are lower as a result. The lower RVEDV contributes to improvement of ventricular energetics as described below.

#### Influence on ventricular energetics

Diastolic regurgitation from PA to RV occurs when a non-valved RV-PA shunt is used. It is possible that the diastolic regurgitation may increase ventricular preload and impair ventricular energetics compared to the valved RV-PA shunt. However, the present study demonstrated that use of both the valved and non-valved RV-PA shunts eliminated systemic to pulmonary diastolic run-off and improved mechanical efficiency (SW/PVA) to the same extent. Compared to the 3.5-mm SPS model, the lower RVEDV in both the 5.0-mm valved and 6.0 mm non-valved RV-PA shunt models contributed to decreasing PVA (−27.2 and −18.0%, respectively) and increasing mechanical efficiency (+5.3 and +9.2%, respectively). Therefore, the influence of diastolic regurgitation associated with the non-valved RV-PA shunt may be small from the viewpoint of ventricular energetics. Because PVA correlates significantly with myocardial oxygen consumption [24], decreased PVA results in reduced myocardial oxygen demand. The present results suggest that both RV-PA shunts reduce myocardial oxygen demand.

This advantage of both RV-PA shunts in ventricular energetics may be associated with the RV ejection pattern through the RV-PA shunts. With the SPS, RV has to pump the blood to a higher pressure system i.e., the systemic circulation. This limits the duration of RV ejection and requires higher RV systolic pressure. However, with both the RV-PA shunts, the systemic and pulmonary arteries originate separately from the RV. The RV ejects blood steadily via the RV-PA shunt to the pulmonary circulation that has a relatively low pressure (Fig. 2). This fact may contribute to the decreased SW and PVA when using the valved and non-valved RV-PA shunts.

#### Advantage of RV-PA shunt

The higher diastolic SAP obtained from using a RV-PA shunt has been reported to improve coronary blood supply [1]. However, under physiological conditions, coronary blood flow depends on myocardial oxygen demand [25]. The greatest advantage of the RV-PA shunt is that this procedure decreases myocardial oxygen demand through decreasing PVA. The RV-PA shunt is able to maintain systemic circulation at lower oxygen consumption compared to the SPS, implying that the RV-PA shunt requires less coronary blood flow than the SPS to maintain the same

**Table 3** The influence of ventriculotomy on ventricular energetics

	$E_{es,RV}$ (mmHg/ml)	SW (mmHg ml)	PVA (mmHg ml)	Mechanical efficiency (%)
3.5-mm SPS	8.5	905	1,157	78.2
6.0-mm non-valved RV-PA	7.5	827	977	84.7
	6.5	825	1,018	81.1
5.0-mm valved RV-PA	7.5	702	875	80.3
	6.5	698	916	76.2

SPS systemic to pulmonary artery shunt, RV-PA right ventricle to pulmonary artery shunt,  $E_{es,RV}$  end-systolic elastance of right ventricle, SW stroke work, PVA systolic pressure–volume area

systemic circulation. This feature may contribute to the improvement of coronary flow reserve. The RV-PA shunt may have better tolerance to the postoperative myocardial ischemia.

#### Limitations

The present study had some limitations. First, the potential damage of right ventriculotomy was disregarded in the present simulations. Ventricular incision is required to place the valved or non-valved RV-PA shunt. Although ventriculotomy may cause ventricular systolic dysfunction or tricuspid regurgitation, Graham et al. [26] observed no apparent deleterious effects of right ventriculotomy following the Norwood procedure using a RV-PA shunt. Furthermore, our additional simulation suggested that the RV-PA shunt still improved ventricular energetics in spite of the potential damage of ventriculotomy, which decreased the end-systolic elastance of RV ( $E_{es,RV}$ ) from 8.5 to 7.5 mmHg/ml (Table 3). However, mechanical efficiency in the 5.0-mm valved RV-PA shunt would be lower than that in the 3.5-mm SPS when ventriculotomy decreased  $E_{es,RV}$  to 6.5 mmHg/ml.

Second, systemic and pulmonary vascular resistance did not change in the present simulations. Vascular resistance was the same in all three shunt models. The differences in pulsatility of the three procedures may affect vascular resistance. A previous report indicated that a sudden increase in systemic vascular resistance caused circulatory collapse in Norwood patients [27]. Therefore, further analyses on the influence of vascular resistance are required.

Third, inertial effects in the shunt were disregarded in the present study. If we considered flow in the shunt as unsteady flow, inertial effects would have a great impact on

the pressure-drop across the shunt. [28] Then, the length of shunt might become a strong determinant of pressure–flow relationship.

#### Conclusions

The present theoretical analysis indicates that both the valved and non-valved RV-PA shunts maintain adequate pulmonary circulation; as a result, the RV delivers greater SW for a lower PVA, i.e., lower myocardial oxygen consumption. Although the valved RV-PA shunt improves pulmonary blood supply and consequently increases  $Q_p$  and oxygen saturation compared to the non-valved RV-PA shunt, the favorable effects of the two RV-PA shunts on ventricular energetics are equivalent. The non-valved RV-PA shunt reduces PVA and improves mechanical efficiency in spite of the presence of PA to RV regurgitation.

**Acknowledgments** This study was supported by a research project promoted by the Japanese Ministry of Health, Labour and Welfare (H20-katsudo-Shitei-007 and H21-nano-Ippan-005); Grants-in-Aid for Scientific Research (No. 20390462, No. 22791328 and No. 23390415) from the Ministry of Education, Culture, Sports, Science and Technology; and the Industrial Technology Research Grant Program from New Energy and Industrial Technology Development Organization (NEDO) of Japan.

#### References

1. Maher KO, Pizarro C, Gidding SS, Januszewska K, Malec E, Norwood WI Jr, Murphy JD (2003) Hemodynamic profile after the Norwood procedure with right ventricle to pulmonary artery conduit. *Circulation* 108:782–784
2. Bove EL, Migliavacca F, de Leval MR, Balossino R, Pennati G, Lloyd TR, Khambadkone S, Hsia TY, Dubini G (2008) Use of mathematic modeling to compare and predict hemodynamic effects of the modified Blalock–Taussig and right ventricle-pulmonary artery shunts for hypoplastic left heart syndrome. *J Thorac Cardiovasc Surg* 136:312–320.e2
3. Reinhartz O, Reddy VM, Petrossian E, MacDonald M, Lamberti JJ, Roth SJ, Wright GE, Pery SB, Suleman S, Hanley FL (2006) Homograft valved right ventricle to pulmonary artery conduit as a modification of the Norwood procedure. *Circulation* 114:1594–1599
4. Takeuchi K, Murakami A, Takaoka T, Takamoto S (2006) Evaluation of valved saphenous vein homograft as right ventricle-pulmonary artery conduit in modified stage I Norwood operation. *Interact Cardiovasc Thorac Surg* 5:345–348
5. Burkhoff D, Tyberg JV (1993) Why does pulmonary venous pressure rise after onset of LV dysfunction: a theoretical analysis. *Am J Physiol* 265:H1819–H1828
6. Morley D, Litwak K, Ferber P, Spence P, Dowling R, Meyns B, Griffith B, Burkhoff D (2007) Hemodynamic effects of partial ventricular support in chronic heart failure: results of simulation validated with in vivo data. *J Thorac Cardiovasc Surg* 133:21–28
7. Shimizu S, Shishido T, Une D, Kamiya A, Kawada T, Sano S, Sugimachi M (2010) Right ventricular stiffness constant as a predictor of postoperative hemodynamics in patients with



- hypoplastic right ventricle: a theoretical analysis. *J Physiol Sci* 60:205–212
8. Sagawa K, Maughan L, Suga H, Sunagawa K (1988) Cardiovascular interaction. In: Sagawa K, Maughan L, Suga H, Sunagawa K (eds) *Cardiac contraction and the pressure–volume relationship*. Oxford University Press, Oxford
  9. Migliavacca F, Pennati G, Dubini G, Fumero R, Pietrabissa R, Urcelay G, Bove EL, Hsia TY, de Leval MR (2001) Modeling of the Norwood circulation: effects of shunt size, vascular resistances, and heart rate. *Am J Physiol Heart Circ Physiol* 280:H2076–H2086
  10. Huikeshoven F, Coleman TG, Jongsma HW (1980) Mathematical model of the fetal cardiovascular system: the uncontrolled case. *Am J Physiol* 239:R317–R325
  11. Migliavacca F, Dubini G, Pennati G, Pietrabissa R, Fumero R, Hsia TY, de Leval MR (2000) Computational model of the fluid dynamics in systemic-to-pulmonary shunts. *J Biomech* 33:549–557
  12. Young DF, Tsai FY (1973) Flow characteristics in models of arterial stenoses. I. Steady flow. *J Biomech* 6:395–410
  13. Chang AC, Kulik TJ, Hickey PR, Wessel DL (1993) Real-time gas-exchange measurement of oxygen consumption in neonates and infants after cardiac surgery. *Crit Care Med* 21:1369–1375
  14. Norwood WI, Lang P, Hansen DD (1983) Physiologic repair of aortic atresia-hypoplastic left heart syndrome. *N Engl J Med* 308:23–26
  15. Pizarro C, Malec E, Maher KO, Januszewska K, Gidding SS, Murdison KA, Baffa JM, Norwood WI (2003) Right ventricle to pulmonary artery conduit improves outcome after stage I Norwood for hypoplastic left heart syndrome. *Circulation* 108:II155–II160
  16. Sano S, Ishino K, Kawada M, Arai S, Kasahara S, Asai T, Masuda Z, Takeuchi M, Ohtsuki S (2003) Right ventricle-pulmonary artery shunt in first-stage palliation of hypoplastic left heart syndrome. *J Thorac Cardiovasc Surg* 126:504–509
  17. Yamashiro M, Morita K, Uno Y, Shinohara G, Hashimoto K (2011) Modified Norwood procedure with a handmade downsizing valved right ventricle-to-pulmonary artery conduit. *Gen Thorac Cardiovasc Surg* 59:30–33
  18. Bradley SM, Simsic JM, McQuinn TC, Habib DM, Shirali GS, Atz AM (2004) Hemodynamic status after the Norwood procedure: a comparison of right ventricle-to-pulmonary artery connection versus modified Blalock–Taussig shunt. *Ann Thorac Surg* 78:933–941
  19. Azakie A, Martinez D, Sapru A, Fineman J, Teitel D, Karl TR (2004) Impact of right ventricle to pulmonary artery conduit on outcome of the modified Norwood procedure. *Ann Thorac Surg* 77:1727–1733
  20. Hoffman GM, Ghanayem NS, Kampine JM, Berger S, Mussatto KA, Litwin SB, Tweddell JS (2000) Venous saturation and the anaerobic threshold in neonates after the Norwood procedure for hypoplastic left heart syndrome. *Ann Thorac Surg* 70:1515–1520
  21. Hoffman GM, Tweddell JS, Ghanayem NS, Mussatto KA, Stuth EA, Jaquis RD, Berger S (2004) Alteration of the critical arteriovenous oxygen saturation relationship by sustained afterload reduction after the Norwood procedure. *J Thorac Cardiovasc Surg* 127:738–745
  22. Caspi J, Pettitt TW, Mulder T, Stopa A (2008) Development of the pulmonary arteries after the Norwood procedure: comparison between Blalock–Taussig shunt and right ventricular-pulmonary artery conduit. *Ann Thorac Surg* 86:1299–1304
  23. Malec E, Januszewska K, Kolcz J, Mroczek T (2003) Right ventricle-to-pulmonary artery shunt versus modified Blalock–Taussig shunt in the Norwood procedure for hypoplastic left heart syndrome—influence on early and late haemodynamic status. *Eur J Cardiothorac Surg* 23:728–733
  24. Suga H, Yasumura Y, Nozawa T, Futaki S, Igarashi Y, Goto Y (1987) Prospective prediction of O<sub>2</sub> consumption from pressure-volume area in dog hearts. *Am J Physiol* 252:H1258–H1264
  25. Tune JD, Gorman MW, Feigl EO (2004) Matching coronary blood flow to myocardial oxygen consumption. *J Appl Physiol* 97:404–415
  26. Graham EM, Atz AM, Bradley SM, Scheurer MA, Bandisode VM, Laudito A, Shirali GS (2007) Does a ventriculotomy have deleterious effects following palliation in the Norwood procedure using a shunt placed from the right ventricle to the pulmonary arteries? *Cardiol Young* 17:145–150
  27. Wright GE, Crowley DC, Charpie JR, Ohye RG, Bove EL, Kulik TJ (2004) High systemic vascular resistance and sudden cardiovascular collapse in recovering Norwood patients. *Ann Thorac Surg* 77:48–52
  28. Young DF, Tsai FY (1973) Flow characteristics in models of arterial stenoses. II. Unsteady flow. *J Biomech* 6:547–559